Neurotoxicology 73 (2019) 120–131

Contents lists available at ScienceDirect

Neurotoxicology

journal homepage: www.elsevier.com/locate/neuro

Full Length Article

Acute expression of the transcription factor Nrf2 after treatment with quinolinic acid is not induced by oxidative stress in the rat striatum

Carlos Alfredo Silva-Islas[a], María Elena Chánez-Cárdenas[a], Diana Barrera-Oviedo[b], María Elena Ibarra-Rubio[c], Perla D. Maldonado[a,*]

[a] Laboratorio de Patología Vascular Cerebral, Instituto Nacional de Neurología y Neurocirugía Manuel Velasco Suárez. Insurgentes Sur 3877, La Fama, Tlalpan, 14269, CDMX, México
[b] Departamento de Farmacología, Facultad de Medicina, Universidad Nacional Autónoma de México, Av Universidad 3000, Coyoacán, 04510, CDMX, México
[c] Departamento de Biología, Facultad de Química, Universidad Nacional Autónoma de México, Av Universidad 3000, Coyoacán, 04510, CDMX, México

ARTICLE INFO

Keywords:
Nrf2
Keap1
p62
DPP3
Quinolinic acid
Brain

ABSTRACT

Quinolinic acid (QUIN) is an excitotoxic and pro-oxidant molecule used in the study of neurodegenerative disorders because it reproduces certain biochemical characteristics present in these diseases. The use of antioxidant molecules in the QUIN model reduces cellular damage through the nuclear factor erythroid 2-related to factor 2 (Nrf2) pathway. The Nrf2 transcription factor is considered the master regulator of antioxidant genes expression, and its activation occurs by an increase in the reactive oxygen species (ROS) levels or in the presence of electrophilic compounds. However, Nrf2 activation also occurs in an oxidative stress-independent process caused by the disruption of the Keap1-Nrf2 complex by the direct interaction of Keap1 with certain proteins, such as DPP3 and p62. The aim of this study was to evaluate the effect of QUIN on Nrf2 activation over short periods of time. QUIN administration increased Nrf2 activation at 30 min in the striatum without increasing ROS production or modifying the redox cellular state. Moreover, QUIN increased Keap1 and Nrf2 nuclear levels and increased the protein-protein interaction between Keap1 and DPP3 and Keap1 and p62 30 min after QUIN administration. Finally, we found that Nrf2 activation primarily occurs in striatal neurons. Our results show that QUIN administration in vivo stimulates Nrf2 expression and activation in the absence of oxidative stress primarily in neurons and increases the interaction of p62 and DPP3 with Keap1, which could participate in Nrf2 activation.

1. Introduction

Quinolinic acid (QUIN) is an endotoxin produced in the human brain through the kynurenine pathway, which is the primary pathway for the production of NAD^+ and $NADP^+$ by tryptophan catabolism (Braidy et al., 2009). QUIN treatment is used as an excitotoxic/pro-oxidant model to study neurodegeneration. QUIN stimulates the N-methyl-D-aspartate receptors (NMDAr), producing an increase in Ca^{2+} influx and activating enzymes associated with reactive oxygen species (ROS) production and cellular damage, finally leading to cellular death (Aguilera et al., 2007; Maldonado et al., 2010; Pérez-Severiano et al., 2004; Santamaría et al., 2001). There are reports indicating that the intrastriatal administration of 240 nmol of QUIN increases hydroxyl radical ($^{\cdot}OH$) levels at 1 h (Santamaría et al., 2001), lipoperoxidation and superoxide anion radical ($O_2^{\cdot -}$) at 2 h (Maldonado et al., 2010; Santamaría and Rios, 1993), the activity of calcium-dependent nitric oxide synthase at 3 h (Aguilera et al., 2007), protein oxidation at 6 h (Colín-González et al., 2013; Santana-Martinez et al., 2014) and decreases glutathione levels at 4 h (Cruz-Aguado et al., 2000; Santamaría et al., 2001; Santana-Martínez et al., 2014). All of this evidence suggests a pro-oxidant effect of QUIN starting at least 1 h after its striatal administration; however, the pro-oxidant capacity of QUIN at times less than 1 h has not been evaluated.

The nuclear factor erythroid 2-related to factor 2 (Nrf2) is a transcription factor that regulates the cellular redox state (reviewed in Hayes and Dinkova-Kostova, 2014). Nrf2 regulates approximately 1055 genes, including proteins and phase 2 enzymes, antioxidant enzymes and proteins involved in cellular development, metabolism, immune system and cellular signaling (Malhotra et al., 2010).

Nrf2 activation is a highly regulated process (Papp et al., 2012). Kelch-like ECH-associated protein 1 (Keap1) regulates the cellular levels of Nrf2 by sequestering and retaining Nrf2 in the cytoplasm

* Corresponding author.
E-mail address: maldonado.perla@gmail.com (P.D. Maldonado).

https://doi.org/10.1016/j.neuro.2019.03.003
Received 28 November 2018; Received in revised form 26 February 2019; Accepted 10 March 2019
Available online 12 March 2019
0161-813X/

through the interaction of the ETGE and DLG motifs in Nrf2 and the Kelch domain in Keap1, causing the ubiquitination and subsequent degradation of Nrf2 by the 26S proteasome (McMahon et al., 2006). Nrf2 is activated by two mechanisms. In the canonical pathway, free radicals and electrophilic compounds induce the release of Nrf2 from Keap1 (reviewed in Hayes and Dinkova-Kostova, 2014; Surh et al., 2008). In the more recently described non-canonical pathway, Nrf2 activation occurs independently of free radicals or electrophilic compounds (reviewed in Hayes and Dinkova-Kostova, 2014). Ho et al. (2005) reported that tetrafluoroethylcysteine activates Nrf2 in the absence of oxidative stress. Moreover, some non-electrophilic molecules, such as tetrahydroisoquinoline, thiopyrimidine, naphthalene, carbazone or urea, can interact with Keap1, preventing Nrf2 sequestration (Richardson et al., 2015). Other studies report that some proteins can interact with Keap1 and prevent Keap1-Nrf2 complex formation. Liu et al. (2007) reported that the phosphotyrosine-independent ligand for the Lck SH2 domain of 62 kDa (p62 or SQSTM1) and dipeptidyl peptidase 3 (DPP3) can activate the Nrf2-ARE pathway in an oxidative stress-independent manner in the neuroblastoma cell line IMR-32 and in mouse-derived primary cortical neurons.

DPP3 is a zinc aminopeptidase able to hydrolyze the N-terminus of oligopeptides containing 3–10 amino acid residues (reviewed in Prajapati and Chauhan, 2011). DPP3 has an ETGE motif, similar to Nrf2, through which it interacts with Keap1. DPP3 can compete with Nrf2 for Keap1 binding. An increase in DPP3 levels decreases Nrf2 ubiquitination and increases its activation. Accordingly, if DPP3 levels decrease, Nrf2 activation is down-regulated (Hast et al., 2013).

Additionally, p62 is a protein that acts as a receptor to selective autophagy of ubiquitinated proteins, organelles and microtubules that are sequestered by phagosomes (Katsuragi et al., 2015). p62 has a DPSTGE motif, similar to the ETGE motif present in Nrf2, which enables the p62-Keap1 interaction. This interaction increases when the mTORC1 complex and the mitogen-activated protein kinase kinase kinase 7 (TAK1) phosphorylate the Ser351 of DPSTGE motif (Hashimoto et al., 2016). There are reports indicating that overexpression of p62 increases the nuclear translocation and activation of Nrf2 in the absence of oxidative stress. Moreover, the p62-Keap1 interaction promotes Keap1 degradation via autophagy (Hashimoto et al., 2016; Lau et al., 2010).

In this study, we evaluated the effect of QUIN administration in vivo on Nrf2 activation over short periods of time. We determined that QUIN induces Nrf2 activation at 30 min in a ROS-independent pathway, primarily in striatal neurons, and increases the Keap1-DPP3 and Keap1-p62 interaction. These data suggest the possible participation of p62 and DPP3 proteins in QUIN-induced Nrf2 activation at 30 min, possibly through the non-canonical pathway.

2. Experimental procedure

2.1. Reagents

Quinolinic acid (QUIN) was purchased from Spectrum. 2´,7´-dichlorofluorescein diacetate (DCF-DA), 2´,7´-dichlorofluorescein (DCF), dihydroethidium (DHE), salmon testes DNA, Hoechst, bovine serum albumin (BSA), N-succinyl-Leu-Tyr-7-amido-4-methyl coumarin, reduced glutathione (GSH), oxidized glutathione (GSSG), glutathione reductase (GR), β-Nicotinamide adenine dinucleotide 2´-phosphate reduced (NADPH), 1-chloro-2,4-dinitrobenzene (CDNB), 2,3-naphthalenedicarboxaldehyde (NDA), o-phthaldehyde, N-ethylmaleimide (NEM), p-formaldehyde (PFA), phosphatase inhibitor cocktail 3, mowiol and mouse anti-α-tubulin (T9026) antibody were obtained from Sigma (St. Louis, MO, USA). Protein A/G plus agarose (sc-2003), rabbit anti-Nrf2 (H300; sc-13032), goat anti-Nrf2 (T-19; sc-30915), rabbit anti-Keap1 (H-190; sc-33569), goat anti-Keap1 (E-20; sc-15246) and mouse anti-PCNA (P-10; sc-56) antibodies were obtained from Santa Cruz Biotechnology (Santa Cruz, CA, USA). Donkey-anti rabbit IgG horseradish peroxidase-conjugate (711-035 − 152) and donkey-anti mouse IgG horseradish peroxidase-conjugate (715-035 − 150) antibodies were from Jackson ImmunoResearch Laboratories Inc. (Jennersville, PA, USA). Rabbit anti-p62 (ab101266), rabbit anti-DPP3 (ab133735), mouse anti-GFAP (ab10062), donkey-anti rabbit IgG Alexa Fluor 488 (ab150073) and donkey-anti mouse IgG Alexa Fluor 594 (ab150108) antibodies were obtained from Abcam (Cambridge, MA, USA). Mouse anti-NeuN (MAB377) antibody was purchased from Millipore (Temecula, CA, USA). The TransAM Nrf2 ELISA kit was from Active Motif (Carlsbad, CA, USA). All other reagents were obtained from other known commercial local sources.

2.2. Animals

One hundred and eighty male Wistar rats (280–320 g) were obtained from the bioterium of the School of Medicine of the National Autonomous University of Mexico. Animals were housed under controlled light conditions (12 h light/dark cycles) and temperature (25 °C ± 3 °C) in an acrylic box (4 rats per cage) with food (Laboratory Rodent Diet 5001; PMI Feeds Inc., Richmond, IN, USA) and water ad libitum. All procedures with animals were carried out strictly according to the National Institutes of Health Guide for the Care and Use of Laboratory Animals and the Local Guidelines on the Ethical Use of Animals from the Health Ministry of Mexico (NOM-062-ZOO − 1999 SAGARPA). INNN 44/15 project. All efforts were made to optimize the number of animals used and to minimize their suffering.

2.3. Experimental design

Animals were randomly divided into three groups (n = 4) as follows: 1) isotonic saline solution group (Saline); 2) 120 nmol of QUIN group (QUIN 120); and 3) 240 nmol of QUIN group (QUIN 240). Animals were sacrificed 15, 30 and 60 min and 3 and 24 h after administration of saline or QUIN, and the nuclear enriched fraction was obtained for the evaluation of Nrf2 activation by ELISA (Fig. 1A).

Because the major activation of Nrf2 was observed 30 min after QUIN administration, subsequent experiments were performed at this time. First, we evaluated whether Nrf2 activation is a dose-response effect after QUIN administration. For this, animals were divided into six groups (n = 4) as follows: 1) isotonic saline solution group (Saline); 2) 15 nmol of QUIN group (QUIN 15); 3) 30 nmol of QUIN group (QUIN 30); 4) 60 nmol of QUIN group (QUIN 60); 5) 120 nmol of QUIN group (QUIN 120); and 6) 240 nmol of QUIN group (QUIN 240). The nuclear enriched fraction was obtained for the evaluation of Nrf2 activation by ELISA (Fig. 1A, dotted square).

Finally, animals were randomly divided into three groups (n = 4–8) as follows: 1) isotonic saline solution group (Saline); 2) 120 nmol of QUIN group (QUIN 120); and 3) 240 nmol of QUIN group (QUIN 240). Independent groups of animals were used to evaluate: 1) ROS production by DCF assay; 2) ROS production by DHE assay, NADPH oxidase (NOX) and xanthine oxidase (XO) activity; 3) calpain activity; 4) protein localization by immunofluorescence; 5) total protein levels by western blot and protein-protein interaction by immunoprecipitation; 6) nuclear protein levels by western blot; and 7) redox cellular state by GSH and GSSG levels and the enzyme activity of GR, glutathione peroxidase (GPx), γ-glutamyl cysteine ligase (GCL), catalase (CAT), glutathione S-transferase (GST) and glucose 6-phosphate dehydrogenase (G6PDH) (Fig. 1B). The protein concentration was determined by the Lowry method.

2.4. Quinolinic acid injection

Animals were anesthetized with sodium pentobarbital (40 mg/kg *ip*) and placed in stereotaxic equipment from Stoelting Co. (Wood Dale, IL, USA). Animals received 1 μL of isotonic saline solution or QUIN with a Hamilton syringe (Hamilton Co., Reno, NV, USA) in the right striatum

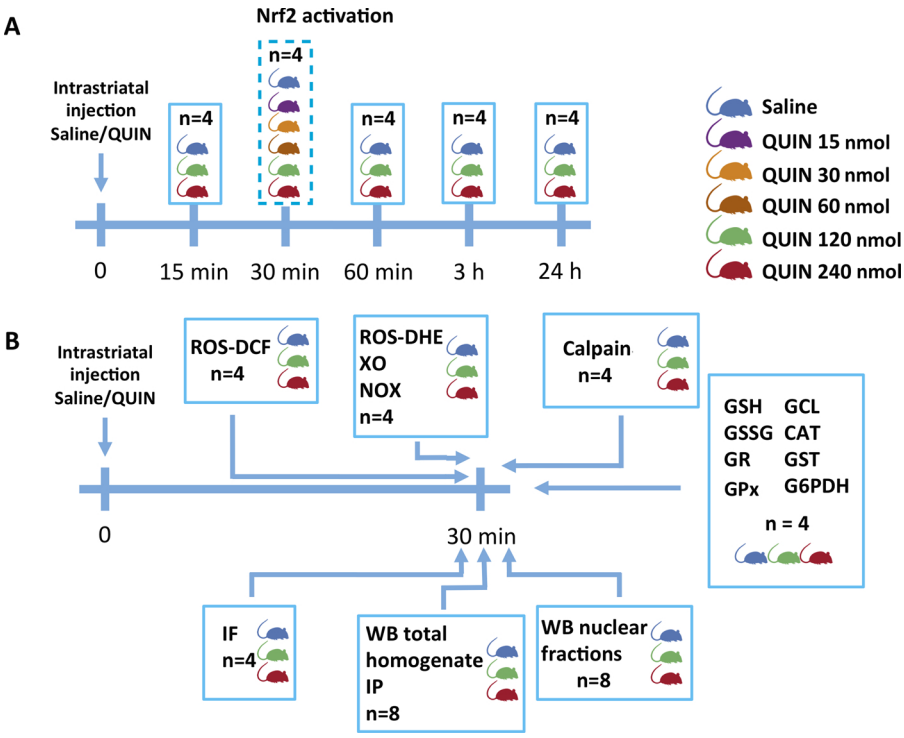

Fig. 1. Experimental design. **A)** Nrf2 activation was evaluated by ELISA after isotonic saline solution (Saline) or quinolinic acid (QUIN 15, 30, 60, 120 and 240 nmol) administration at 15, 30 and 60 min and 3 and 24 h. **B)** The subsequent experiments were performed at 30 min. Individual boxes represent an independent group of animals for each evaluation. Rats in different colors represent the specific groups studied in each experiment. The number of animals used in all the groups studied in each experiment (n) is indicated. ROS-DCF: Reactive oxygen species by dichlorofluorescein, ROS-DHE: Reactive oxygen species by dihydroethidium, XO: xanthine oxidase, NOX: NADPH oxidase, GSH: reduced glutathione, GSSG: oxidized glutathione, GR: glutathione reductase, GPx: glutathione peroxidase, GCL: γ-glutamyl cysteine ligase, CAT: catalase, GST: glutathione S-transferase, G6PDH: glucose 6-phosphate dehydrogenase, IF: immunofluorescence, WB: Western blot, IP: immunoprecipitation.

according to the following stereotaxic coordinates: +0.5 mm anterior to bregma, -2.6 mm lateral to bregma and -4.5 mm ventral to dura (Paxinos and Watson, 1998; Santana-Martínez et al., 2014).

2.5. Preparation of total homogenates

Samples were homogenized in cold lysis buffer (10 mM Tris HCl pH 7.6, 15 mM NaCl, 0.25 mM sucrose, 1 μg/mL aprotinin, 1 μg/mL leupeptin, 1 μg/mL pepstatin A, 1 mM PMSF and 1% Triton X100) and centrifuged at 10,621 x g for 20 min at 4 °C. The supernatants were used in western blotting and immunoprecipitation assays and in the measurement of the glutathione levels and enzyme activities of GR, GCL, GST, GPx, CAT and G6PDH.

2.6. Nuclear enriched fraction

Samples were homogenized in HB buffer (20 mM HEPES pH 7.4, 1 mM EDTA, 1 mM DTT, 1 mM PMSF, 1 μg/mL pepstatin A, 1 μg/mL aprotinin, 1 μg/mL leupeptin and 1X phosphatase inhibitor cocktail 3) plus 0.5% Nonidet P40 and incubated on ice for 15 min. The homogenates were centrifuged at 850 x g for 10 min at 4 °C, and the pellets were resuspended in HB buffer, incubated on ice for 10 min followed by the addition of 15 μL of 10% Nonidet P40 and incubated for 5 min. The samples were centrifuged at 14,000 x g for 2 min at 4 °C, and the pellets were resuspended in complete lysis buffer (TransAM, Nrf2), vortexed on ice and incubated for 30 min at 150 rpm. The samples were vortexed for 30 s and centrifuged at 14,000 x g for 10 min at 4 °C, and the supernatant (nuclear enriched fraction) was collected and used in a western blot analysis and ELISA.

2.7. ROS detection by DCF

The right striatum was incubated in dissect solution (9.84 mM HEPES pH 7.3, 136.7 mM NaCl, 5 mM KCl, 0.1 mM Na_2HPO_4, 0.2 mM KH_2PO_4, 16.6 mM D-glucose and 21.9 mM sucrose) plus 0.25% trypsin for 15 min at 37 °C. Tissues were passed through syringes of different calibers (20 G, 21 G, 22 G and 25 G) and incubated with 20 μM DCF-DA for 30 min at 37 °C. Samples were washed 3 times with PBS, lysed in lysis buffer (19.62 mM KH_2PO_4, 30.38 mM K_2HPO_4 pH 7.4 and 1% Triton X100) and sonicated. Fluorescence was measured at λ 488 nm of excitation and λ 515 nm of emission in a fluorescence plate reader (Synergy HT, BioTek, Winooski, VT, USA) and compared with a standard curve using DCF. The results were expressed as pmol of DCF/μg of protein.

2.8. ROS detection by DHE

ROS production by DHE was determined as previously reported by Maldonado et al. (2010). We used an exogenous positive control with healthy striatum plus an $O_2^{\cdot -}$ generator system (2 mM xanthine and 0.5 U/mL XO) and an endogenous positive control with kidneys from rats treated with 1 dose of 15 mg/kg of potassium dichromate for 24 h. ROS production was expressed as DHE fluorescence/mg of protein vs control.

2.9. NOX and XO activity

Sixty microliters of the supernatant remaining from ROS evaluation by DHE assay were transferred to a 96-well plate, and 1.8 μL of 1 mM DHE, 4.4 μL of 10 mg/mL salmon testes DNA, 11.38 μL of distilled water and 8.62 μL of 1 mM NADPH or 8.62 μL of 1 mM xanthine were added to measure the NOX and XO activities, respectively. The plate was incubated for 30 min at 37 °C in darkness, and the fluorescence intensity was measured at λ 480 nm of excitation and λ 610 nm of emission in a fluorescence plate reader (Synergy HT, Biotek, Winooski, VT, USA). NOX and XO activities were expressed as DHE fluorescence/mg of protein vs control.

2.10. Calpain activity

The calpain activity was quantified as an indirect indicator of intracellular calcium levels. The striata were isolated and homogenized in 500 μL of hypotonic buffer (25 mM HEPES pH 7.4, 5 mM $MgCl_2$, 1.3 mM EDTA and 1 mM EGTA) plus 1 mM DTT, 0.1% Triton X100, 1 μg/mL aprotinin and 1 μg/mL pepstatin A. The homogenates were centrifuged at 10,621 x *g* for 20 min at 4 °C, and 15 μL of supernatants

were transferred to a fluorescence 96-well plate, and 135 µL of buffer A (63 mM imidazol − HCl pH 7.3, 10 mM 2-mercaptoetanol, 1 mM EDTA and 10 mM EGTA) was added. The plate was incubated for 10 min at 37 °C followed by the addition of 1.52 µL of 10 mM N-succinyl-Leu-Tyr-7-amido-4-methyl coumarin, and the fluorescence was measured at λ 380 nm of excitation and λ 460 nm of emission every min for 40 min. The activity of calpain was expressed as the change in fluorescence (ΔAUF)/min/mg of protein.

2.11. GR activity

Fifty microliters of samples were added to 950 µL of reaction mix (62 mM KH_2PO_4, 38 mM Na_2HPO_4 pH 7.6, 0.5 mM EDTA, 1.1 mM GSSG and 1 mM NADPH), and the absorbance was measured immediately at 340 nm. Absorbance was recorded every 30 s for 3 min. Phosphate buffer (62 mM KH_2PO_4, 38 mM Na_2HPO_4 pH 7.6) was used as a blank. The activity was calculated from the slope of these lines (µmoles of NADPH oxidized per min) using a molar extinction coefficient of NADPH (6.22×10^{-3} M^{-1} cm^{-1}). GR activity was expressed as U/mg of protein.

2.12. GST activity

Eighty microliters of samples were added to 850 µL of phosphate buffer (41.8 mM KH_2PO_4, 8.2 mM Na_2HPO_4 pH 6.5) and 20 µL of 50 mM GSH dissolved in phosphate buffer pH 6.5. The reaction was initiated by the addition of 50 µL of 20 mM CDNB dissolved in DMSO. Absorbance at 340 nm was recorded every 30 s for 3 min. Blank reaction was prepared using distilled water replacing homogenates. The activity was calculated from the slope of these lines (µmoles of GS-DNB formed per min) using a molar extinction coefficient of the conjugate oxidized glutathione-2,4-dinitrobenzene (GS-DNB, 9.6×10^{-3} M^{-1} cm^{-1}). GST activity was expressed as U/mg of protein.

2.13. GCL activity

Twenty microliters of samples were added to 50 µL of reaction mix (400 mM Tris-base, 20 mM L-glutamic acid, 2 mM EDTA, 20 mM boric acid, 2 mM L-serine, 10 mM $MgCl_2$ and 40 mM ATP). Reaction was initiated by the addition of 50 µL of 2 mM L-cysteine dissolved in TES-SB buffer (20 mM Tris-base pH 8.0, 1 mM EDTA, 250 mM sucrose, 2 mM L-serine and 20 mM boric acid), and samples were incubated for 20 min at 37 °C. The reaction was stopped by the addition of 50 µL of 200 mM sulfosalicylic acid followed by incubation at 4 °C for 20 min. Samples were centrifuged at 1300 x *g* for 5 min at 4 °C, and 20 µL of supernatant was transferred to a 96-well plate. Then, 180 µL of 10 mM NDA was added to the supernatants followed by incubation for 15 min in darkness at room temperature to allow the formation of the NDA-Glu-Cys complex (NDA-ɣ-GC). The fluorescence intensity of the NDA-ɣ-GC complex was measured at λ 485 nm of excitation and λ 535 nm of emission in a fluorescence plate reader (Synergy HT, Biotek, Winooski, VT, USA). In parallel, each sample was treated to remove the basal GSH levels. In these tubes, L-cysteine was added after sulfosalicylic acid. Fluorescence levels were compared with a GSH standard curve, and GCL activity was expressed as µg NDA-ɣ-GC/mg protein.

2.14. G6PDH activity

Ninety microliters of samples were added to 470 µL of buffer A (55 mM Tris − HCl pH 7.8 and 3.3 mM $MgCl_2$), 20 µL of 6 mM NADP dissolved in buffer A and 20 µL of 100 mM glucose-6-phosphate dissolved in buffer A. Absorbance at 340 nm was recorded every 30 s for 6 min. Buffer A was used as a blank. The activity was calculated from the slope of these lines (µmoles of NADPH oxidized per min) using a molar extinction coefficient of NADPH (6.22×10^{-3} M^{-1} cm^{-1}). G6PDH activity was expressed as U/mg of protein.

2.15. CAT activity

Twenty-five microliters of samples were added to 725 µL of reaction mix (6 mM KH_2PO_4, 4 mM Na_2HPO_4 pH 7.0 plus 30 mM H_2O_2), and the absorbance was measured immediately at 240 nm every 15 s for 3 min. The activity was calculated in the time period where the reaction was lineal. A blank reaction with distilled water replacing homogenates was subtracted from each assay. The activity was calculated from the slope of these lines (µmoles of H_2O_2 consumption per min) using a molar extinction coefficient of H_2O_2 (40 M^{-1} cm^{-1}). CAT activity was expressed as U/mg of protein.

2.16. GPx activity

One hundred microliters of samples were added to 800 µL of reaction mix (30 mM KH_2PO_4, 20 mM Na_2HPO_4 pH 7.0, 1 mM EDTA, 1 mM NaN_3, 0.2 mM NADPH, 1 mM GSH and 1 U/mL GR) and incubated for 5 min at room temperature. The reaction started by the addition of 100 µL of 0.25 mM H_2O_2 solution. Absorbance at 340 nm was recorded every 30 s for 3 min. In parallel, the absorbance of an unspecific tube (100 µL of distilled water, 800 µL of reaction mix and 100 µL of 0.25 mM H_2O_2 solution) was measured, and the value was subtracted from each assay. The activity was calculated from the slope of these lines (µmoles of NADPH oxidized per min) using a molar extinction coefficient of NADPH (6.22×10^{-3} M^{-1} cm^{-1}). GPx activity was expressed as U/mg of protein.

2.17. GSH and GSSG levels

GSH levels: 100 µL of the supernatant of total homogenates was added to 900 µL of GSH buffer (0.12 M NaH_2PO_4, 0.26 M Na_2HPO_4 pH 8.0 and 0.006 M EDTA) and was mixed. Twenty microliters of this mix was added to 360 µL of GSH buffer followed by the addition of 20 µL of 1 mg/mL o-phthaldehyde, and the samples were incubated for 15 min at room temperature in darkness. The fluorescence intensity was measured at λ 350 nm of excitation and λ 420 nm of emission in a fluorescence plate reader (Synergy HT, Biotek, Winooski, VT, USA).

GSSG levels: 40 µL of 5 mg/mL NEM was added to 100 µL of supernatant of total homogenates, and the samples were incubated for 30 min at room temperature in the darkness, then 860 µL of 0.1 N NaOH were added. Twenty microliters of this mix was added to 360 µL of 0.1 N NaOH and 20 µL of 1 mg/mL o-phthaldehyde, and the samples were incubated for 15 min at room temperature in darkness. The fluorescence intensity was measured at λ 350 nm of excitation and λ 420 nm of emission in a fluorescence plate reader (Synergy HT, Biotek, Winooski, VT, USA).

Fluorescence levels of GSH and GSSG were compared with a standard curve of GSH and GSSG, respectively. Levels of GSH and GSSG were expressed as µg of GSH/mg of protein or µg of GSSG/mg of protein, respectively.

2.18. Western blot

Fifty micrograms of total homogenate, 80 µg of nuclear enriched fraction or all supernatant from immunoprecipitation were run in polyacrylamide gels and transferred to PVDF membranes. Membranes were blocked with 5% nonfat milk and incubated with primary antibody against goat anti-Nrf2 (1:1000), rabbit anti-p62 (1:5000), rabbit anti-DPP3 (1:10,000), rabbit anti-Keap1 (1:500), mouse anti-α tubulin (1:10,000) or mouse anti-PCNA (1:500) overnight followed by the incubation of the secondary antibody against rabbit (1:10,000), mouse (1:10,000) or goat (1:10,000). Membranes were revealed using an Immobilon Western kit (Millipore Co, Billerica, MA, USA), and images were obtained with a Photodocumenter (Vilber Lourmat, Eberhardzell, Deutschland).

2.19. Immunoprecipitation

Thirty microliters of protein A/G plus agarose were preblocked with 200 µL of 1% BSA for 1 h with agitation. Three hundred micrograms of whole striatum homogenate were added to preblocked protein A/G plus agarose and incubated for 2 h at room temperature with agitation. At the same time, in a second series of tubes one microgram of goat anti-Keap1 antibody was added to preblocked protein A/G plus agarose and incubated for 2 h at room temperature with agitation and washed once with PBS. Samples were centrifuged at 1000 x *g* for 3 min at 4 °C and the supernatant was added to the tubes containing goat anti-Keap1 antibody and protein A/G plus agarose. Tubes were incubated overnight with agitation at 4 °C and washed with wash buffer (10 mM Tris − HCl pH 7.4, 1 mM EDTA, 1 mM EGTA, 150 mM NaCl, 0.2 mM Na_3VO_4, 1 mM PMSF, 1 µg/mL pepstatin A, 1 µg/mL aprotinin, 1 µg/mL leupeptin, and 1% Triton X100). Samples were resuspended in 25 µL of Laemmli buffer, boiled for 8 min and loaded in polyacrylamide gel. Western blotting was performed as previously described.

2.20. Immunofluorescence

Animals were perfused transcardially with isotonic saline solution plus heparin (5000 U/L) followed by 4% PFA solution. Brains were removed and placed in a 4% PFA solution plus 10% sucrose for 24 h, then placed in 4% PFA plus 20% sucrose for 24 h and finally in 4% PFA plus 30% sucrose for 24 h. Brains were embedded in Tissue-Tek, and 10 µm slices were obtained using a cryostat (GMI, Ramsey, MN, USA). Sections were boiled in 10 mM sodium citrate pH 6 for 45 min, cooled at room temperature and incubated in 0.1 M glycine for 1 h at room temperature followed by permeabilization with PBS plus 0.1% Triton X100 for 30 min. Sections were blocked with 3% fetal bovine serum for 1 h at room temperature followed by the incubation of primary antibody against rabbit anti-Nrf2 (1:25) or rabbit anti-p62 (1:500) overnight at 4 °C. Sections were incubated with the second primary antibody against mouse anti-GFAP (1:500) or mouse anti-NeuN (1:100) plus Hoechst (1:1000) overnight at 4 °C followed by incubation with secondary antibody anti-mouse Alexa fluor 594 (1:250) and anti-rabbit Alexa fluor 488 (1:250) for 2 h at room temperature and the addition of 10 µL of mowiol. Finally, sections were visualized in a fluorescence microscope Nikon E 200 (Nikon, Melville, NY, USA) using a 40X objective.

2.21. Nrf2 activation

The active Nrf2 bound to the ARE sequence (Nrf2 activation) was determined by ELISA according to the manufacturer's instructions (TransAM Nrf2 Active Motif) using the nuclear enriched fraction. The results were expressed as optical density (OD) at 450 nm/mg protein vs saline.

2.22. Statistical analysis

All data are presented as the mean ± SEM. Data were analyzed by one-way ANOVA and post hoc Tukey´s test using Prism 5.0 software (GraphPad, San Diego, CA. USA). Values of $P < 0.05$ were considered to be statistically significant.

3. Results

3.1. QUIN activates Nrf2 at 30 min

QUIN was unable to induce Nrf2 activation at 15 min, whereas at 30 min, Nrf2 activation increased compared to the saline group. At 60 min, Nrf2 activation returned to basal levels and remained at these levels at 3 and 24 h compared to the saline group (Fig. 2A).

Additionally, we evaluated whether Nrf2 activation by QUIN is a dose-dependent process at 30 min. QUIN at 15 nmol was unable to induce the activation of Nrf2; however, with 30 nmol, the Nrf2 activation increased, reaching a maximum activation level with 60 nmol of QUIN and remaining with 120 and 240 nmol of QUIN (Fig. 2B). Based on this evidence and the commonly used doses of QUIN in this model, we selected 120 and 240 nmol doses of QUIN at 30 min in subsequent experiments.

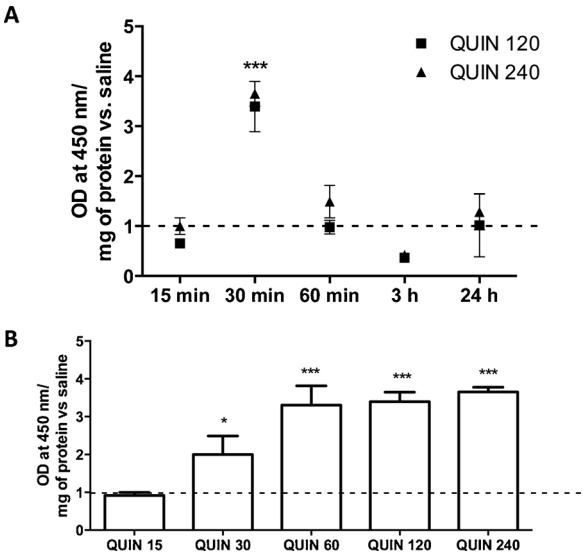

Fig. 2. Effect of quinolinic acid (QUIN) on Nrf2 activation in the striatum. **A)** Animals were administered in the right striatum with 1 µL of isotonic saline solution (saline group, dotted line, normalized to 1) or QUIN (120 and 240 nmol), and samples were collected at 15, 30 and 60 min and 3 and 24 h. Nuclear enriched fractions of striatum were used to evaluate the active Nrf2 bound to the ARE sequence in the ELISA plate (Nrf2 activation). **B)** Animals were administered with 1 µL of isotonic saline solution (saline group, dotted line, normalized to 1) or QUIN (15, 30, 60, 120 and 240 nmol) in the right striatum, and samples were collected at 30 min. Nuclear enriched fractions of striatum were used to evaluate Nrf2 activation by ELISA. Data are expressed as the mean ± SEM of four animals per group. *P < 0.05 and ***P < 0.001 vs. Saline group.

3.2. QUIN does not increase ROS production

QUIN is a molecule widely used as an excitotoxic/pro-oxidant model, and there is considerable evidence suggesting its role as an oxidative stress inducer. For this reason, we evaluated ROS production as a possible mechanism of Nrf2 activation by quantification of DCF fluorescence 30 min after the administration of 120 and 240 nmol of QUIN. QUIN (120 and 240 nmol) was unable to increase ROS levels at 30 min compared to the saline group (Fig. 3A); to confirm these results, we evaluated ROS levels using the oxidation of DHE fluorescent probe. QUIN (120 and 240 nmol) was unable to increase ROS levels at 30 min compared to the saline group. We used the $O_2^{-\cdot}$ generator system xanthine/XO and kidneys from rats administered with potassium dichromate as positive controls (Fig. 3B).

3.3. QUIN does not induce oxidative stress

To corroborate the absence of ROS production observed previously (Fig. 3), we measured other markers of cell redox status, such as GSH and GSSG levels, the activity of phase 2 and antioxidant enzymes and the activity of NOX, XO and calpain (Table 1). As expected, QUIN did not modify GSH levels compared to the saline group, as well as the GSSG levels and the GSH/GSSG ratio. Also, QUIN was unable to change the activity of GR, GPx, GCL and CAT at 30 min; nevertheless, an increase in the GST activity and a slight decrease in the activity of G6PDH

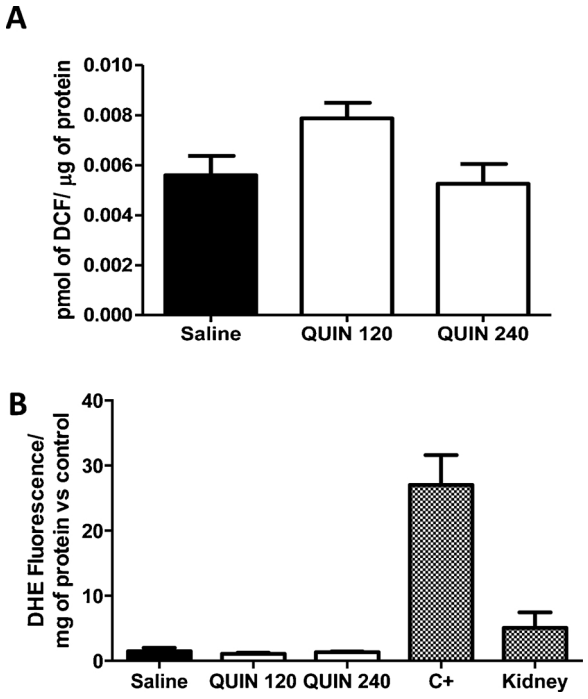

Fig. 3. Effect of quinolinic acid (QUIN) on ROS production in the striatum using **A)** dichlorofluorescein (DCF) and **B)** dihydroethidium (DHE) assays at 30 min. Animals were administered in the right striatum with 1 µL of isotonic saline solution (saline) or QUIN (120 and 240 nmol). In **B:** an exogenous positive control (C+) using a superoxide anion generator system (xanthine/XO) and an endogenous positive control (Kidney) using the kidney of rats treated for 24 h with 15 mg/kg of potassium dichromate were used. Data are expressed as the mean ± SEM of four animals per group.

with 240 nmol of QUIN were observed. Additionally, no changes were observed in the NOX and XO activities at 30 min after QUIN administration. Finally, the activity of calpain increased with QUIN 120 nmol at 30 min (Table 1). Taken together, these results suggest that QUIN does not change the redox cellular state.

3.4. QUIN modifies the cellular localization of Nrf2 and Keap1

QUIN induced an increase in Nrf2 activation at 30 min (Fig. 2); however, as observed in Fig. 3, QUIN was unable to induce an increase in ROS production at this experimental time, indicating that Nrf2 activation occurs in the absence of ROS, possibly through the non-canonical pathway. To test this possibility, we evaluated the changes in Nrf2, Keap1, p62, and DPP3 protein levels and their nuclear translocation in response to QUIN (120 and 240 nmol) at 30 min. In total homogenates, no changes were observed in Nrf2, p62 and DPP3 levels after QUIN administration (Fig. 4A, B, D and E); nevertheless, Keap1 levels increased with 240 nmol of QUIN (Fig. 4A and C).

Nuclear translocation of Nrf2 and Keap1 was tested, and it increased in response to 240 nmol QUIN (Fig. 5A, B and C). Nuclear levels of p62 showed a tendency to increase in response to 240 nmol of QUIN; however, there was no significant difference (Fig. 5A and D). Nuclear levels of DPP3 were not evaluated because this protein does not have a nuclear localization signal.

3.5. QUIN increases DPP3-Keap1 and p62-Keap1 protein-protein interactions

Since Nrf2 activation increased in the absence of ROS production, we hypothesized that the increase in Nrf2 activation occurs by the disruption of the Keap1-Nrf2 complex. To support this hypothesis, an immunoprecipitation assay was performed to evaluate whether Keap1 interacts with DPP3 or p62 30 min after QUIN administration (15, 30, 60, 120 and 240 nmol). QUIN (15–240 nmol) induced an increase in DPP3 and p62 interaction with Keap1 in a dose-dependent manner (Fig. 6); however, the major increase was observed using 120 and 240 nmol of QUIN (Fig. 6). These results indicate that QUIN activates Nrf2 in the absence of oxidative stress and increases DPP3 and p62 interaction with Keap1 in striatal tissue, suggesting the participation of DPP3 and p62 in Nrf2 activation.

3.6. QUIN induces p62 and Nrf2 expression mainly in neurons

To determine in which type of striatal cells occurs Nrf2 expression in response to QUIN, the Nrf2 and p62 levels in neurons and astrocytes were measured by immunofluorescence. A marked localization of Nrf2 in the nucleus of neurons was observed (Fig. 7A), while in astrocytes, Nrf2 expression was scarce (Fig. 7B), suggesting that Nrf2 activation is primarily carried out in neurons (Fig. 7A and 7B). The p62 expression was observed primarily in the nucleus of neurons; however, a low signal was also observed in the cytoplasm, specifically in the perinuclear area, in animals administered with saline and QUIN (120 and 240 nmol) (Fig. 8A). In contrast, the p62 expression in astrocytes was low (Fig. 8B).

Table 1
Effect of quinolinic acid (QUIN) on the cellular redox state at 30 min.

	Group		
Determination	Saline	QUIN 120	QUIN 240
GSH (µg/mg protein)	0.4295 ± 0.01564	0.4359 ± 0.01548	0.4084 ± 0.03882
GSSG (µg/mg protein)	0.5710 ± 0.05161	0.4968 ± 0.02924	0.5399 ± 0.05017
GSH/GSSG ratio	0.7697 ± 0.07061	0.8900 ± 0.07833	0.7674 ± 0.06886
GR (U/mg protein)	0.0019 ± 0.0001	0.0019 ± 0.0002	0.0023 ± 0.0003
GPx (U/mg protein)	0.0013 ± 0.0002	0.0013 ± 0.0001	0.0014 ± 0.0001
GCL (µg NDA-ɣ-GC/mg protein)	0.0827 ± 0.0031	0.0857 ± 0.0147	0.0851 ± 0.0085
CAT (U/mg protein)	$0.0004 \pm 5.7 \times 10^{-5}$	$0.0003 \pm 2.3 \times 10^{-5}$	$0.0003 \pm 4.0 \times 10^{-5}$
GST (U/mg protein)	0.0025 ± 0.0003	0.0029 ± 0.0002	0.0055 ± 0.0004***
G6PDH (U/mg protein)	0.0071 ± 0.0002	0.0058 ± 0.0002	0.0043 ± 0.0005*
NOX (Fluorescence DHE/mg protein vs control)	1.0380 ± 0.20450	0.8001 ± 0.09974	1.2220 ± 0.29520
XO (Fluorescence DHE/mg protein vs control)	1.1630 ± 0.15050	0.8598 ± 0.04896	1.2290 ± 0.15250
Calpain (ΔAUF/min/mg protein)	32.20 ± 0.5351	43.17 ± 1.3900*	37.47 ± 2.55700

Data are expressed as the mean ± SEM of four animals per group. *P < 0.05 and ***P < 0.001 vs. Saline group.
GSH: reduced glutathione, GSSG: oxidized glutathione, GR: glutathione reductase, GPx: glutathione peroxidase, GCL: ɣ-glutamyl cysteine ligase, NDA-ɣ-GC: NDA-Glu-Cys complex, CAT: catalase, GST: glutathione S-transferase, G6PDH: glucose 6-phosphate dehydrogenase, NOX: NADPH oxidase, XO: xanthine oxidase, DHE: dihydroethidium, ΔAUF: change in fluorescence.

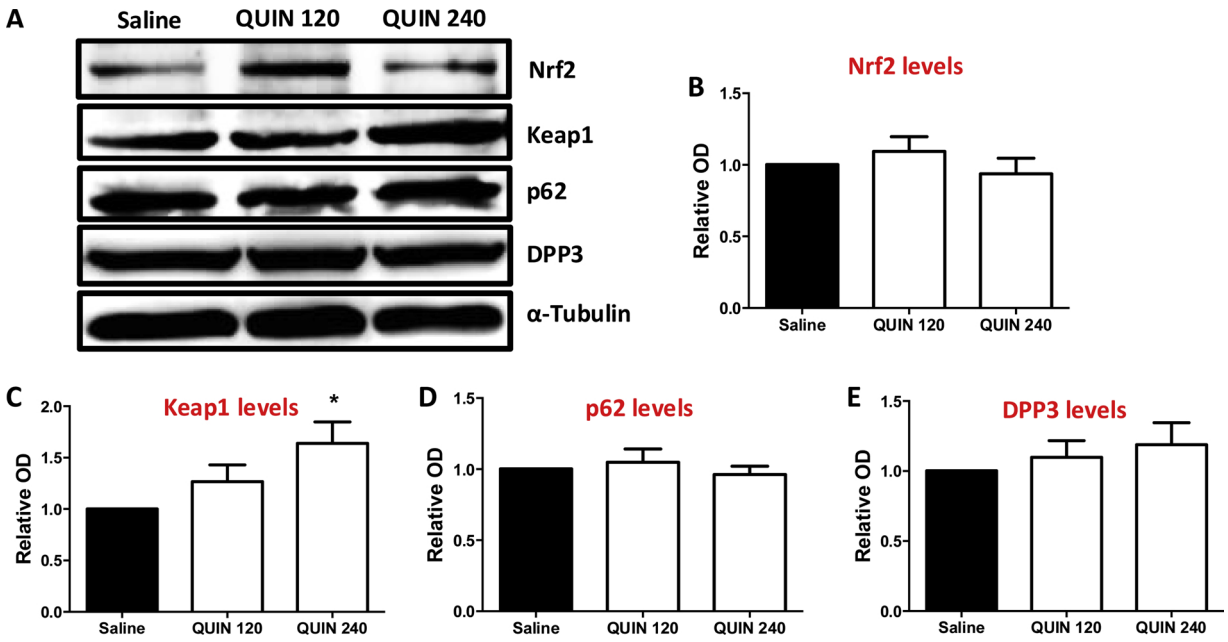

Fig. 4. Effect of quinolinic acid (QUIN) on Nrf2, Keap1, p62 and DPP3 levels at 30 min in striatum total homogenate. Animals were administered with 1 μL of isotonic saline solution (Saline) or QUIN (120 and 240 nmol) in the right striatum, and western blotting was performed. Representative images of WB analysis **(A)** and densitometric quantification of all samples analyzed for Nrf2 **(B)**, Keap1 **(C)**, p62 **(D)** and DPP3 **(E)** proteins are shown. Data are expressed as the mean ± SEM of eight animals per group. *P < 0.05 vs. saline group.

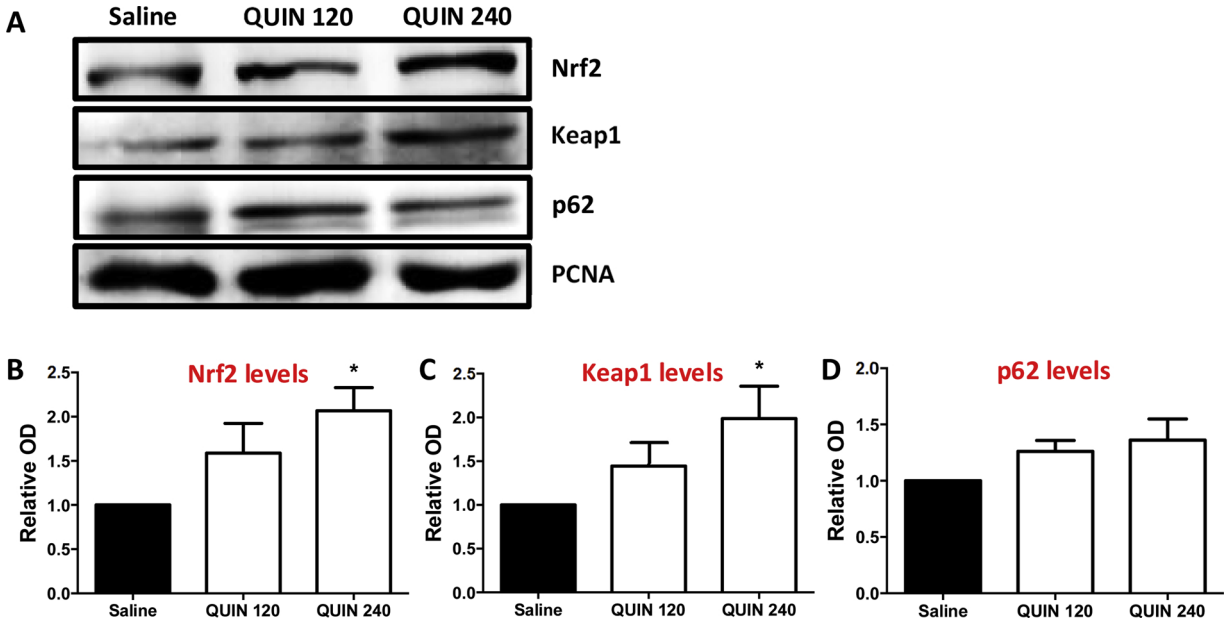

Fig. 5. Effect of quinolinic acid (QUIN) on the nuclear amount of Nrf2, Keap1 and p62 proteins in striatum at 30 min. Animals were administered in the right striatum with 1 μL of isotonic saline solution (Saline) or QUIN (120 and 240 nmol). The nuclear enriched fraction was isolated, and western blotting was performed. Representative images of WB analysis **(A)** and densitometric quantification of all samples analyzed for Nrf2 **(B)**, Keap1 **(C)** and p62 **(D)** proteins are shown. Data are expressed as the mean ± SEM of eight animals per group. *P < 0.05 vs. saline group.

4. Discussion

The QUIN model is widely used in the study of excitotoxic and oxidant events associated with neurological diseases. The intrastriatal administration of QUIN (120–240 nmol) induces cellular damage to the middle spiny neurons through the activation of NMDAr, resulting in an increase in intracellular Ca^{2+} levels and ROS generation. Previous studies have measured ROS effects using in vivo QUIN administration in periods varying from 1 h to 7 days; however, at periods shorter than 1 h, the ROS effects are poorly studied. Moreover, antioxidants such as sulforaphane and curcumin show protection against the damage induced by QUIN due to their ability to decrease ROS levels through Nrf2 activation, indicating the importance of this pathway (Santana-Martínez et al., 2014; Singh and Kumar, 2016).

To understand whether Nrf2 participates as a possible mechanism of protection after acute QUIN administration (15 min to 24 h), we studied the effect of QUIN on Nrf2 activation. Our results show that Nrf2 activation (binding of nuclear Nrf2 to the ARE sequence) occurs 30 min after QUIN in a dose-dependent response between 15–60 nmol of QUIN, similar to previous studies (Huang et al., 2012; Lee et al., 2012). A

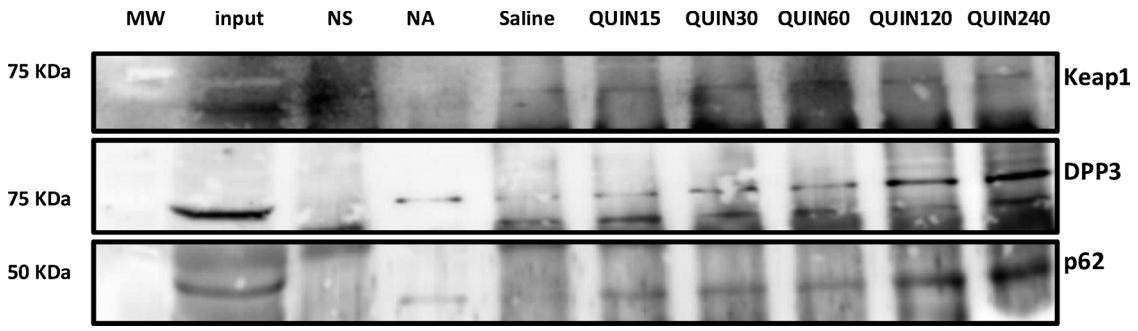

Fig. 6. Effect of quinolinic acid (QUIN) on the protein-protein interaction of Keap1 with DPP3 and p62 in the striatum at 30 min. Animals were administered in the right striatum with 1 µL of isotonic saline solution (saline) or different doses of QUIN (15, 30, 60, 120 and 240 nmol). An immunoprecipitation assay was performed on the total homogenate of four animals per group, to evaluate the interaction between Keap1 and DPP3 or p62. Keap1 was immunoprecipitated, and the Keap1, DPP3 and p62 western blot analyses were performed. Molecular weight marker (MW); negative control of IP without sample (NS); negative control of IP without antibody (NA).

maximum Nrf2 activation was observed with 120 and 240 nmol of QUIN. This fast Nrf2 activation suggests a possible protective mechanism to counteract the damage induced by QUIN at times over 30 min, since Nrf2 is implicated in the expression of around 1055 genes including those coding for antioxidant enzymes, phase II enzymes, or other proteins involved in the metabolism, the immune system and the cellular signaling (Malhotra et al., 2010). Previous reports have described a similar effect, that is, a rapid Nrf2 nuclear translocation after different stimuli, such as 4-hydroxynonenal (Huang et al., 2012), tunicamycin (Cullinan et al., 2003), pantoprazole (Lee et al., 2012) and tert-butylhydroquinone (Alarcón-Aguilar et al., 2014).

Based on the evidence that QUIN is an excitotoxic and pro-oxidant molecule (Colín-González et al., 2013; Santamaría and Rios, 1993; Santamaría et al., 2001; Santana-Martínez et al., 2014), we expected that Nrf2 activation observed 30 min after QUIN administration could be related to an increase in oxidative state. However, the ROS levels did not show changes at these conditions. Moreover, no changes in the main oxidative stress markers GSH, GSSG levels and GSH/GSSG ratio were observed, indicating that QUIN is unable to induce ROS production before 30 min. Additionally, the activity of antioxidant (CAT, GPx, GR, GCL and G6PDH) and phase 2 (GST) enzymes was measured to evaluate their possible participation in ROS remotion. The activity of the antioxidant enzymes CAT, GPx, GR and GCL did not change, whereas GST activity increased and G6PDH activity decreased 30 min following treatment with QUIN (240 nmol). The biological significance of these changes is unknown. We propose that the increase in GST activity and the decrease in G6PDH activity are independent of both, oxidative stress and Nrf2 activation, but more experiments must be done to elucidate their role after QUIN exposure at this time. GST is a typical phase 2 detoxification enzyme that conjugates GSH with substrate molecules in order to promote its clearance. However, it is also involved in other processes such as intracellular binding and transport of hydrophobic compounds, catalysis of some steps in the synthesis of leukotrienes, prostaglandins and steroid hormones, as well as cell signaling regulation (Pljesa-Ercegovac et al., 2018). Regarding G6PDH, this enzyme has an indirect antioxidant function, since it produces the NADPH used by GR in order to reduce GSSG to GSH (Stanton, 2012).

Additionally, we determined the NOX and XO activities, since these enzymes are the primary ones responsible for increasing ROS levels after an excitotoxic event, such as QUIN treatment (Maldonado et al., 2010). QUIN administration does not increase the activity of NOX and XO, indicating that the absence of ROS at 30 min is a consequence of QUIN's inability to induce the activity of these enzymes. NOX and XO activities increase in response to cytoplasmic Ca^{2+} levels, and the lack of change in its enzyme activity could be associated with the inability of QUIN to increase cytoplasmic Ca^{2+} levels at 30 min. To explore this mechanism involved in the absence of ROS production, we evaluated the intracellular Ca^{2+} levels, since the increase in ROS production after excitotoxic events is a consequence of the increase in Ca^{2+} levels. The intracellular Ca^{2+} levels were measured indirectly by recording the calpain activity, a Ca^{2+}–dependent enzyme (reviewed in Yildiz-Unal et al., 2015), as an indicator of NMDAr activation. The calpain activity did not show changes in response to QUIN, indicating that the absence in ROS production is due to a poor increase in cytoplasmic Ca^{2+} at 30 min. The lack of cytoplasmic Ca^{2+} increment after QUIN exposure was previously observed in striatal slices at 30 min (Pierozan et al., 2014), corroborating that QUIN is unable to increase the cytoplasmic Ca^{2+} levels and subsequent ROS levels at 30 min. It is important to note that these results do not indicate that QUIN is unable to induce ROS production; rather, they indicate that ROS production is an event that occurs after 30 min (Vandresen-Filho et al., 2015).

These results together with the Nrf2 observations indicate that Nrf2 activation at 30 min occurs in the absence of ROS and the oxidative stress state. In previous works, Liu et al. (2007) observed that Nrf2 activation in cells from the central nervous system is carried out through the non-canonical pathway by an increase in DPP3 and p62 protein levels and in the absence of oxidative stress. For this reason, we evaluated the participation of DPP3 and p62 in the activation of Nrf2 at 30 min after QUIN.

The total levels of Nrf2, Keap1, p62 and DPP3 and their nuclear translocation were evaluated, except that of DPP3, since these proteins participate in non-canonical Nrf2 activation. The total levels of Nrf2 at 30 min did not increase in response to QUIN; however, nuclear translocation of Nrf2 increased only in response to 240 nmol of QUIN. Our results correlate with previous observations that indicate that sulforaphane and quercetin, two well-described Nrf2 inducers, increase Nrf2 nuclear translocation without changes in the total Nrf2 protein content (Xue et al., 2015). Furthermore, we did not observe an increase in Nrf2 nuclear levels after 120 nmol of QUIN, despite the activation observed with this dose. A similar response was previously reported in primary cultured astrocytes after tert-butylhydroquinone administration (Alarcón-Aguilar et al., 2014). These findings indicate that Nrf2 activation is not only dependent on its nuclear accumulation, since not all Nrf2 translocated to the nucleus is able to bind to the ARE sequence (Velichkova and Hasson, 2005). In fact, the binding of Nrf2 to ARE sequences depends on several other factors, such as the heterodimerization of Nrf2 with small Maf proteins (reviewed in Surh et al., 2008), the acetylation of Lys residues in Nrf2 (Kawai et al., 2011) or the repression of Bach proteins through its binding to ARE sequences (Ishikawa et al., 2005; Oyake et al., 1996).

We observed an increase in total levels and nuclear translocation of Keap1 using 240 nmol of QUIN. An increase in Keap1 nuclear translocation was previously observed in cell culture treated with diethylmaleate, sulforaphane and tert-butylhydroquinone (Velichkova and Hasson, 2005), which is associated with post-activation repression of Nrf2 through its nuclear export in a Keap1-dependent manner and its

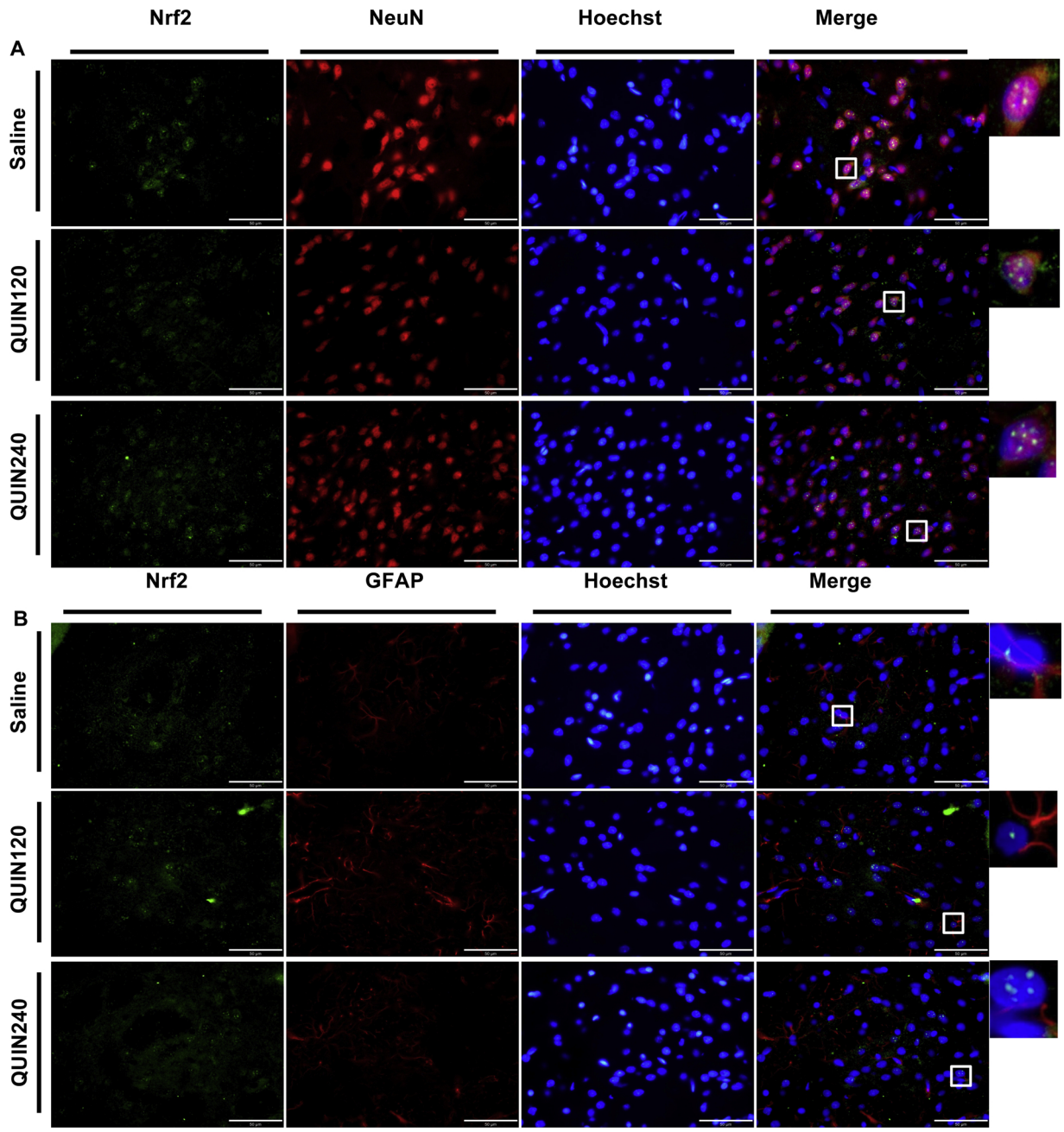

Fig. 7. Effect of quinolinic acid (QUIN) on the localization of Nrf2 in neurons and astrocytes. Animals were administered with 1 µL of isotonic saline solution (Saline) or QUIN (120 and 240 nmol) in the right striatum at 30 min. Brains were collected and fixed, and 10-µm coronal sections were obtained. Immunofluorescence was performed, and microphotographs were taken to identify in **A)** Nrf2 (green), NeuN (red) and nucleus (blue); and in **B)** Nrf2 (green), GFAP (red) and nucleus (blue). Scale bars represent 50 µm. The white box shows the magnified positive cells on the right. Microphotographs are representative images of four animals per group (For interpretation of the references to colour in this figure legend, the reader is referred to the web version of this article).

subsequent degradation (Sun et al., 2007). This finding could explain why at over longer time periods (1, 3 and 24 h), we did not observe Nrf2 activation.

The activation of Nrf2 through the non-canonical pathway depends on the interaction of Keap1 with DPP3 or p62 proteins, disrupting the Keap1-Nrf2 complex. For this reason, we evaluated whether the protein-protein interaction of Keap1 with DPP3 or p62 participates in Nrf2 activation. We observed an increase in Keap1-DPP3 and Keap1-p62 interaction in a dose-response manner 30 min after QUIN. Based on this evidence, our results indicate that Nrf2 activation occurs in an oxidative stress-independent manner and suggest the participation of DPP3 and p62 in Nrf2 activation possibly through the non-canonical pathway at 30 min in the QUIN model. This finding correlates with previous reports that showed an increase in the protein-protein interaction between Keap1 and DPP3 and between Keap1 and p62, promoting nuclear translocation and activation of Nrf2 in cell culture (Hast et al., 2013; Lau et al., 2010). However, to date, this interaction has not been observed in in vivo models. Our work also describes the increase in Nrf2 activation as an endogenous response, in contrast to other works in which Nrf2 activation depends on the overexpression of DPP3 and p62 (Hashimoto et al., 2016; Hast et al., 2013; Lau et al., 2010; Liu et al., 2007).

There is a considerable discrepancy regarding the cell type in which Nrf2 is activated; several works report that Nrf2 activation occurs only in neurons (Tanaka et al., 2011); in astrocytes, neurons and microglia (Dang et al., 2012; Takagi et al., 2014); or primarily in astrocytes

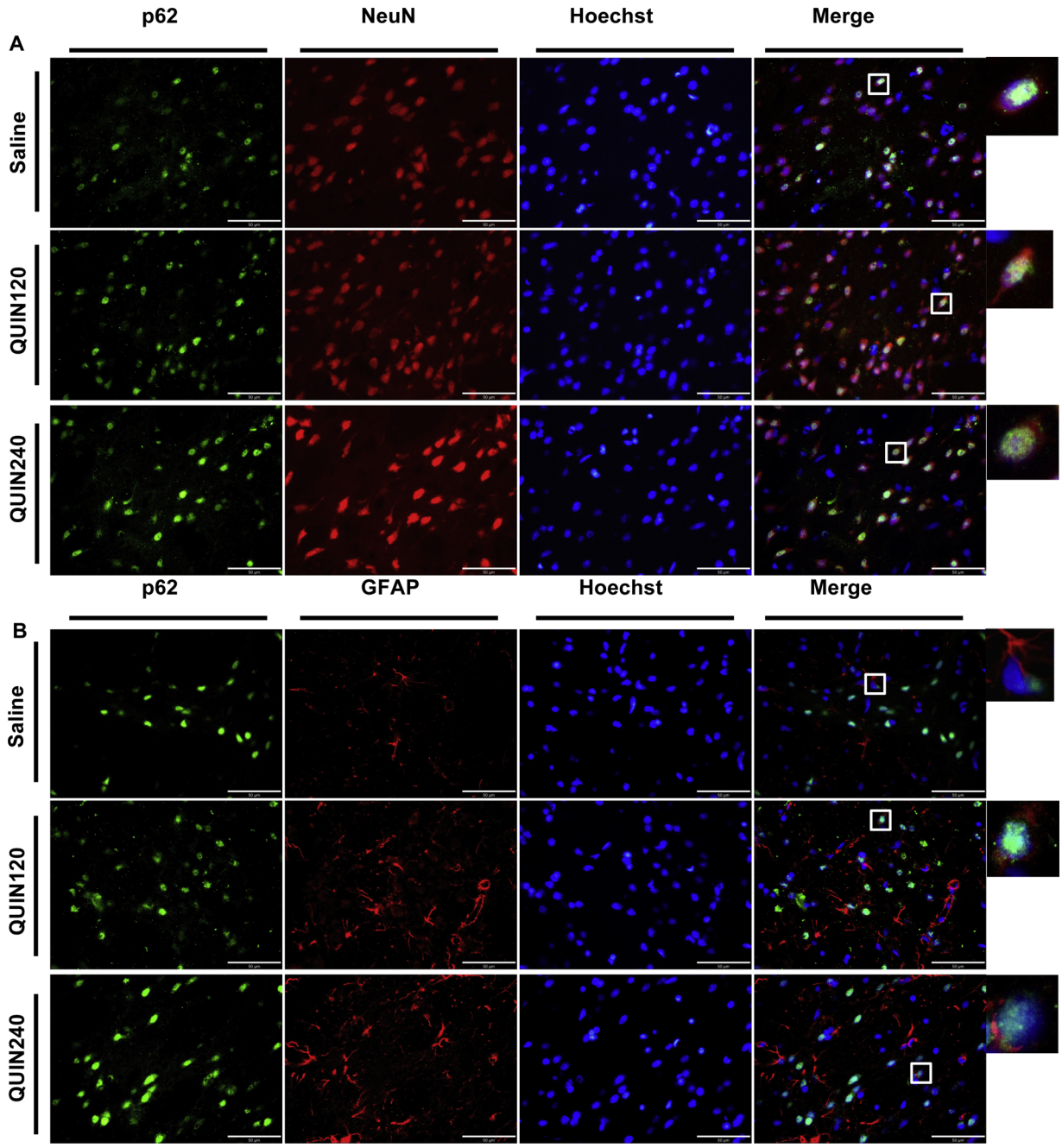

Fig. 8. Effect of quinolinic acid (QUIN) on the localization of p62 in neurons and astrocytes. Animals were administered with 1 μL of isotonic saline solution (Saline) or QUIN (120 and 240 nmol) in the right striatum at 30 min. Brains were collected and fixed and 10-μm coronal sections were obtained. Immunofluorescence was performed, and microphotographs were taken to identify in **A)** p62 (green), NeuN (red) and nucleus (blue); and in **B)** p62 (green), GFAP (red) and nucleus (blue). Scale bars represent 50 μm. The white box shows the magnified positive cells on the right. Microphotographs are representative images of four animals per group (For interpretation of the references to colour in this figure legend, the reader is referred to the web version of this article).

(Habas et al., 2013; Jimenez-Blasco et al., 2015; Kraft et al., 2004). Our results show that Nrf2 is expressed primarily in neuronal cells, at least at 30 min following treatment with QUIN. This result is relevant, since it indicates that neurons trigger a response to defend and preserve themselves against noxious stimuli, such as QUIN, thereby maintaining the functionality of the affected brain region.

p62 is a protein expressed mainly in the cytoplasm (Sanchez et al., 1998) due to its function in autophagy (Zatloukal et al., 2002). However, p62 distribution varies depending on the cell/tissue studied. For example, in HeLa cells (Bjørkøy et al., 2005) and in tissues derived from lung and gastric carcinoma (Schläfli et al., 2015) the localization of p62 is mainly cytoplasmic although a reduced number of cells also show its presence in the nucleus. Our immunofluorescence results show that p62 expression is primarily in the neurons nucleus at least at 30 min following treatment with QUIN. The accumulation of p62 in the nucleus has also been reported in oral mucosa tissues derived from healthy persons (Liu et al., 2014), in brain tissue of R6/2 mice (Nagaoka et al., 2004) and in HT1080 cells after cefotaxime treatment (Noguchi et al., 2018). The function of p62 in the nucleus has not been thoroughly elucidated to date. However, p62 has two nuclear localization signals and one nuclear export signal in its structure which allow it to shuttle between cytoplasm and nucleus (Pankiv et al., 2010) and might mediate the crosstalk between autophagy and the UPS in DNA repair (Hewitt et al., 2016).

Based on our results, we suggest that the interaction between DPP3 and Keap1 in the cytoplasm leads to the release of Nrf2 from Keap1 enabling the nuclear translocation and activation of Nrf2. On the other hand, p62 interacts with Keap1 in the nucleus, increasing Nrf2 nuclear levels. This nuclear p62-Keap1 association could prevent Nrf2-Keap1 interaction, and in consequence, the nuclear export of Nrf2-Keap1 complex, which also may explain the observed Nrf2 activation at 30 min. In accordance to our proposal, Sun et al. (2007) demonstrated that in MDA-MB-231 cells treated with tert-butylhydroquinone occur the nuclear translocation of Keap1 in order to dissociate Nrf2 from the ARE sequence, and the ulterior export of this Nrf2-Keap1 complex to the cytoplasm for the Nrf2 ubiquitination and degradation. Another possibility is that p62 could bind Keap1 promoting their nuclear translocation, decreasing cytoplasmic Keap1 levels and releasing Nrf2, which in turn, could be translocated to the nucleus and bind ARE sequences. These hypothesis, however, need to be evaluated.

5. Conclusions

The present study demonstrates that Nrf2 activation in vivo at 30 min after QUIN administration occurs in the absence of ROS production, in an oxidative stress-independent process that take place primarily in neurons of the striatum. This Nrf2 activation could be through the non-canonical pathway, since QUIN induces an increase in Keap1-DPP3 and Keap1-p62 interaction.

Funding

This work was supported by a CONACyT grant [number 241655] to PDM. Carlos Alfredo Silva-Islas received a scholarship from CONACyT [number 276541].

Declaration of interest

None.

Transparency document

The Transparency document associated with this article can be found in the online version.

Acknowledgements

Carlos Alfredo Silva-Islas is a PhD student from Programa de Maestría y Doctorado en Ciencias Bioquímicas, Universidad Nacional Autónoma de México (UNAM) and this publication is derived from his doctoral thesis.

References

Aguilera, P., Chánez-Cárdenas, M.E., Floriano-Sánchez, E., Barrera, D., Santamaría, A., Sánchez-González, D.J., Pérez-Severiano, F., Pedraza-Chaverrí, J., Jiménez, P.D., 2007. Time-related change in constitutive and inducible nitric oxide synthases in the rat striatum in model of Huntington´s disease. Neurotoxicology 28, 1200–1207. https://doi.org/10.1016/j.neuro.2007.07.010.

Alarcón-Aguilar, A., Luna-López, A., Ventura-Gallegos, J.L., Lazzarini, R., Galván-Arzate, S., González-Puertos, V.Y., Morán, J., Santamaría, A., Königsberg, M., 2014. Primary cultured astrocytes from old rats are capable to activate the Nrf2 response against MPP+ toxicity after tBHQ pretreatment. Neurobiol. Aging 35, 1901–1912. https://doi.org/10.1016/j.neurobiolaging.2014.01.143.

Bjørkøy, G., Lamark, T., Brech, A., Outzen, H., Perander, M., Overvatn, A., Stenmarl, H., Johansen, T., 2005. p62/SQSTM1 forms protein aggregates degraded by autophagy and has a protective effect on huntingtin-induced cell death. J. Cell Biol. 171, 603–614. https://doi.org/10.1083/jcb.200507002.

Braidy, N., Grant, R., Adams, S., Brew, B.J., Guillemin, G.J., 2009. Mechanism for quinolinic acid cytotoxicity in human astrocytes and neurons. Neurotox. Res. 16, 77–86. https://doi.org/10.1007/s12640-009-9051-z.

Colín-González, A.L., Orozco-Ibarra, M., Chánez-Cárdenas, M.E., Rangel-López, E., Santamaría, A., Pedraza-Chaverrí, J., Barrera-Oviedo, D., Maldonado, P.D., 2013. Heme oxigenase-1 (HO-1) upregulation delays morphological and oxidative induced in an excitotoxic/pro-oxidant model in the rat striatum. Neuroscience 231, 91–101. https://doi.org/10.1016/j.neuroscience.2012.11.031.

Cruz-Aguado, R., Francis-Turner, L., Díaz, C.M., Antúnez, I., 2000. Quinolinic acid lesion induces changes in rat striatal glutathione metabolism. Neurochem. Int. 37, 53–60. https://doi.org/10.1016/s0197-0186(99)00165-5.

Cullinan, S.B., Zhang, D., Hannink, M., Arvisais, E., Kaufman, R.J., Diehl, J.A., 2003. Nrf2 is a direct PERK substrate and effector of PERK-dependent cell survival. Mol. Cell. Biol. 23, 7198–7209. https://doi.org/10.1128/mcb.23.20.7198-7209.2003.

Dang, J., Brandenburg, L.O., Rosen, C., Fragoulis, A., Kipp, M., Pufe, T., Beyer, C., Wruck, C.J., 2012. Nrf2 expression by neurons, astroglia, and microglia in the cerebral cortical penumbra of ischemic rats. J. Mol. Neurosci. 46, 578–584. https://doi.org/10.1016/j.brainres.2010.11.010.

Habas, A., Hahn, J., Wang, X., Margeta, M., 2013. Neuronal activity regulates astrocytic Nrf2 signaling. Proc. Natl. Acad. Sci. U. S. A. 110, 18291–18296. https://doi.org/10.1073/pnas.1208764110.

Hashimoto, K., Simmons, A.N., Kajino-Sakamoto, R., Tsuji, Y., Ninomiya-Tsuji, J., 2016. TAK1 regulates the Nrf2 antioxidant system through modulating p62/SQSTM1. Antioxid. Redox Signal. 25, 953–964. https://doi.org/10.1089/ars.2016.6663.

Hast, B.E., Goldfarb, D., Mulvaney, K.M., Hast, M.A., Siesser, P.F., Yan, F., Hayes, D.N., Major, M.B., 2013. Proteomic analysis of ubiquitin ligase KEAP1 reveals associated proteins that inhibit NRF2 ubiquitination. Cancer Res. 73, 2199–2210. https://doi.org/10.1158/0008-5472.CAN-12-4400.

Hayes, J.D., Dinkova-Kostova, A.T., 2014. The Nrf2 regulatory network provides an interface between redox and intermediary metabolism. Trends Biochem. Sci. 39, 199–218. https://doi.org/10.1016/j.tibs.2014.02.002.

Hewitt, G., Carroll, B., Sarallah, R., Correia-Melo, C., Ogrodnik, M., Nelson, G., Otten, E.G., Manni, D., Antrobus, R., Morgan, B.A., von Zglinicki, T., Jurk, D., Seluanov, A., Gorbunova, V., Johansen, T., Passos, J.F., Korolchuk, V.I., 2016. SQSTM1/p62 mediates crosstalk between autophagy and the UPS in DNA repair. Autophagy 12, 1917–1939. https://doi.org/10.1080/15548627.2016.1210368.

Ho, H.K., White, C.C., Fernandez, C., Fausto, N., Kavanagh, T.J., Nelson, S.D., Bruschi, S.A., 2005. Nrf2 activation involves an oxidative-stress independent pathway in tetrafluoroethylcysteine-induced cytotoxicity. Toxicol. Sci. 86, 354–364. https://doi.org/10.1093/toxsci/kfi205.

Huang, Y., Li, W., Kong, A.N., 2012. Anti-oxidative stress regulator NF-E2-related factor 2 mediates the adaptive induction of antioxidant and detoxifying enzymes by lipid peroxidation metabolite 4-hydroxynonenal. Cell Biosci. 2, 40. https://doi.org/10.1186/2045-3701-2-40.

Ishikawa, M., Numazawa, S., Yoshida, T., 2005. Redox regulation of the transcriptional repressor Bach1. Free Radic. Biol. Med. 38, 1344–1352. https://doi.org/10.1016/j.freeradbiomed.2005.01.021.

Jimenez-Blasco, D., Santofimia-Castaño, P., Gonzalez, A., Almeida, A., Bolaños, J.P., 2015. Astrocyte NMDA receptors' activity sustains neuronal survival through a Cdk5-Nrf2 pathway. Cell Death Differ. 22, 1877–1889. https://doi.org/10.1038/cdd.2015.49.

Katsuragi, Y., Ichimura, Y., Komatsu, M., 2015. p62/SQSTM1 functions as a single hub and autophagy adaptor. FEBS J. 282, 4672–4678. https://doi.org/10.1111/febs.13540.

Kawai, Y., Garduño, L., Theodore, M., Yang, J., Arinze, I.J., 2011. Acetylation-deacetylation of the transcription factor Nrf2 (nuclear factor erythroid 2-related factor 2) regulates its transcriptional activity and nucleocytoplasmic localization. J. Biol. Chem. 286, 7629–7640. https://doi.org/10.1074/jbc.M110.208173.

Kraft, A.D., Johnson, D.A., Johnson, J.A., 2004. Nuclear factor E2-related factor 2-dependent antioxidant response element activation by tert-butylhydroquinone and sulphoraphane occurring preferentially in astrocytes conditions neurons against oxidative insult. J. Neurosci. 24, 1101–1112. https://doi.org/10.1523/JNEUROSCI.3817-03.2004.

Lau, A., Wang, X.J., Zhao, F., Villeneuve, N.F., Wu, T., Jiang, T., Sun, Z., White, E., Zhang, D.D., 2010. A noncanonical mechanism of Nrf2 activation by autophagy deficiency: direct interaction between Keap1 and p62. Mol. Cell. Biol. 30, 3275–3285. https://doi.org/10.1128/MCB.00248-10.

Lee, H.J., Han, Y.M., Kim, E.H., Kim, Y.J., Hahm, K.B., 2012. A possible involvement of Nrf2-mediated heme oxygenase-1 up-regulation in protective effect of the proton pump inhibitor pantoprazole against indomethacin-induced gastric damage in rats. BMC Gastroenterol. 12, 143. https://doi.org/10.1186/1471-230x-12-143.

Liu, Y., Kern, J.T., Walker, J.R., Johnson, J.A., Schultz, P.G., Luesch, H., 2007. A genomic screen for activators of the antioxidant response element. Proc. Natl. Acad. Sci. U. S. A. 104, 5205–5210. https://doi.org/10.1073/pnas.0700898104.

Liu, J.L., Chen, F.F., Lung, J., Lo, C.H., Lee, F.H., Lu, Y.C., Hung, C.H., 2014. Prognostic significance of p62/SQSTM1 subcellular localization and LC3B in oral squamous cell carcinoma. Br. J. Cancer 111, 944–954. https://doi.org/10.1038/bjc.2014.355.

Maldonado, P.D., Molina-Jijón, E., Villeda-Hernández, J., Galván-Arzate, S., Santamaría, A., Pedraza-Chaverrí, J., 2010. NADP(H) oxidase contributes to neurotoxicity in an excitotoxic/prooxidant model of Huntington´s disease in rats: protective role of apocynin. J. Neurosci. Res. 88, 620–629. https://doi.org/10.1002/jnr.22240.

Malhotra, D., Portales-Casamar, E., Singh, A., Srivastava, S., Arenillas, D., Happel, C., Shyr, C., Wakabayashi, N., Kensler, T.W., Wasserman, W.W., Biswal, S., 2010. Global mapping of binding sites for Nrf2 identifies novel targets in cell survival response through ChIP-Seq profiling and network analysis. Nucleic Acids Res. 38, 5718–5734. https://doi.org/10.1093/nar/gkq212.

McMahon, M., Thomas, N., Itoh, K., Yamamoto, M., Hayes, J.D., 2006. Dimerization of substrate adaptors can facilitate cullin-mediated ubiquitylation of proteins by a "tethering" mechanism. J. Biol. Chem. 281, 24756–24768. https://doi.org/10.1074/jbc.M601119200.

Nagaoka, U., Kim, K., Jana, N.R., Doi, H., Maruyama, M., Mitsui, K., Oyama, F., Nukina, N., 2004. Increased expression of p62 in expanded polyglutamine-expressing cells

and its association with polyglutamine inclusions. J. Neurochem. 91, 57–68. https://doi.org/10.1111/j.1471-4159.2004.02692.x.
Noguchi, T., Suzuki, M., Mutoh, N., Hirata, Y., Tsuchida, M., Miyagawa, S., Hwang, G.W., Aoki, J., Matsuzawa, A., 2018. Nuclear-accumulated SQSTM1/p62-based ALIS act as microdomains sensing cellular stresses and triggering oxidative stress-induced parthanatos. Cell Death Dis. 9, 1193. https://doi.org/10.1038/s41419-018-1245-y.
Oyake, T., Itoh, K., Motohashi, H., Hayashi, N., Hoshino, H., Nishizawa, M., Yamamoto, M., Igarashi, K., 1996. Bach proteins belong to a novel family of BTB-basic leucine zipper transcription factors that interact with MafK and regulate transcription through the NF-E2 site. Mol. Cell. Biol. 16, 6083–6095. https://doi.org/10.1128/mcb.16.11.6083.
Pankiv, S., Lamark, T., Brunn, J.A., Øvervatn, A., Bjørkøy, G., Johansen, T., 2010. Nucleocytoplasmic shuttling of p62/SQSTM1 and its role in recruitment of nuclear polyubiquitinated proteins to promyelocytic leukemia bodies. J. Biol. Chem. 285, 5941–5953. https://doi.org/10.1074/jbc.M109.039925.
Papp, D., Lenti, K., Módos, D., Fazekas, D., Dúl, Z., Türei, D., Földvári-Nagy, L., Nussinov, R., Csermely, P., Korcsmáros, T., 2012. The Nrf2-related interactome and regulome contain multifunctional proteins and fine-tuned autoregulatory loops. FEBS Lett. 586, 1795–1802. https://doi.org/10.1016/j.febslet.2012.05.016.
Paxinos, G., Watson, C., 1998. The Rat Brain in Stereotaxic Coordinates. USA. Academic Press Inc, San Diego Press.
Pérez-Severiano, F., Rodríguez-Pérez, M., Pedraza-Chaverrí, J., Maldonado, P.D., Medina-Campos, O.N., Ortíz-Plata, A., Sánchez-García, A., Villeda-Hernández, J., Galván-Arzate, S., Aguilera, P., Santamaría, A., 2004. S-Allylcysteine, a garlic-derived antioxidant, ameliorates quinolinic acid-induced neurotoxicity and oxidative damage in rats. Neurochem. Int. 45, 1175–1183. https://doi.org/10.1016/j.neuint.2004.06.008.
Pierozan, P., Fernandes, C.G., Dutra, M.F., Pandolfo, P., Ferreira, F., de Lima, B.O., Porciúncula, L., Wajner, M., Pessoa-Pureur, R., 2014. Biochemical, histopathological and behavioral alterations caused by intrastriatal administration of quinolinic acid to young rats. FEBS J. 281, 2061–2073. https://doi.org/10.1111/febs.12762.
Pljesa-Ercegovac, M., Savic-Radojevic, A., Matic, M., Coric, V., Djukic, T., Radic, T., Simic, T., 2018. Glutathione transferases: potential target to overcome chemoresistance in solid tumors. Int. J. Mol. Sci. 19, E3785. https://doi.org/10.3390/ijms19123785.
Prajapati, S.C., Chauhan, S.S., 2011. Dipeptidyl peptidase III: a multifaceted oligopeptide N-end cutter. FEBS J. 278, 3256–3276. https://doi.org/10.1111/j.1742-4658.2011.08275.x.
Richardson, B.G., Jain, A.D., Speltz, T.E., Moore, T.W., 2015. Non-electrophilic modulators of the canonical Keap1/Nrf2 pathway. Bioorg. Med. Chem. Lett. 25, 2261–2268. https://doi.org/10.1016/j.bmcl.2015.04.019.
Sanchez, P., De Carcer, G., Sandoval, I.V., Moscat, J., Diaz-Meco, M.T., 1998. Localization of atypical protein kinase C isoforms into lysosome-targeted endosomes through interaction with p62. Mol. Cell. Biol. 18, 3069–3080. https://doi.org/10.1128/mcb.18.5.3069.
Santamaría, A., Rios, C., 1993. MK-801, an N-methyl-D-aspartate receptor antagonist, blocks quinolinic acid-induced lipid peroxidation in rat corpus striatum. Neurosci. Lett. 159, 51–54. https://doi.org/10.1016/0304-3940(93)90796-n.
Santamaría, A., Jiménez-Capdeville, M.E., Camacho, A., Rodríguez-Martínez, E., Flores, A., Galván-Arzate, S., 2001. In vivo hydroxyl radical formation after quinolinic acid infusion into rat corpus striatum. Neuroreport 12, 2693–2696. https://doi.org/10.1097/00001756-200108280-00020.
Santana-Martínez, R.A., Galván-Arzáte, S., Hernández-Pando, R., Chánez-Cárdenas, M.E., Avila-Chávez, E., López-Acosta, G., Pedraza-Chaverrí, J., Santamaría, A., Maldonado, P.D., 2014. Sulforaphane reduces the alteration induced by quinolinic acid: modulation of glutathione levels. Neuroscience 272, 188–198. https://doi.org/10.1016/j.neuroscience.2014.04.043.
Schläfli, A.M., Berezowska, S., Adams, O., Langer, R., Tschan, M.P., 2015. Reliable LC3 and p62 autophagy marker detection in formalin fixed paraffin embedded human tissue by immunohistochemistry. Eur. J. Histochem. 59, 2481. https://doi.org/10.4081/ejh.2015.2481.
Singh, S., Kumar, P., 2016. Neuroprotective activity of curcumin in combination with piperine against quinolinic acid induced neurodegeneration in rats. Pharmacology 97, 151–160. https://doi.org/10.1159/000443896.
Stanton, R.C., 2012. Glucose-6-phosphate dehydrogenase, NADPH, and cell survival. IUBMB Life 64, 362–369. https://doi.org/10.1002/iub.1017.
Sun, Z., Zhang, S., Chan, J.Y., Zhang, D.D., 2007. Keap1 controls postinduction repression of the Nrf2-mediated antioxidant response by escorting nuclear export of Nrf2. Mol. Cell. Biol. 27, 6334–6349. https://doi.org/10.1128/MCB.00630-07.
Surh, Y.J., Kundu, J.K., Na, H.K., 2008. Nrf2 as a master redox switch in turning on the cellular signaling involved in the induction of cytoprotective genes by some chemopreventive phytochemicals. Planta Med. 74, 1526–1539. https://doi.org/10.1055/s-0028-1088302.
Takagi, T., Kitashoji, A., Iwawaki, T., Tsuruma, K., Shimazawa, M., Yoshimura, S., Iwama, T., Hara, H., 2014. Temporal activation of Nrf2 in the penumbra and Nrf2 activator-mediated neuroprotection in ischemia-reperfusion injury. Free Radic. Biol. Med. 72, 124–133. https://doi.org/10.1016/j.freeradbiomed.2014.04.009.
Tanaka, N., Ikeda, Y., Ohta, Y., Deguchi, K., Tian, F., Shang, J., Matsuura, T., Abe, K., 2011. Expression of Keap1-Nrf2 system and antioxidative proteins in mouse brain after transient middle cerebral artery occlusion. Brain Res. 1370, 246–253. https://doi.org/10.1016/j.brainres.2010.11.010.
Vandresen-Filho, S., Martins, W.C., Bertoldo, D.B., Mancini, G., De Bem, A.F., Tasca, C.I., 2015. Cerebral cortex, hippocampus, striatum and cerebellum show differential susceptibility to quinolinic acid-induced oxidative stress. Nuerol. Sci. 36, 1449–1456. https://doi.org/10.1007/s10072-015-2180-7.
Velichkova, M., Hasson, T., 2005. Keap1 regulates the oxidative-sensitive shuttling of Nrf2 into and out of the nucleus via a Crm1-dependent nuclear export mechanisms. Mol. Cell. Biol. 25, 4501–4513. https://doi.org/10.1128/mcb.25.11.4501-4513.2005.
Xue, M., Momiji, H., Rabbani, N., Barker, G., Bretschneider, T., Shmygol, A., Rand, D.A., Thornalley, P.J., 2015. Frequency modulated translocational oscillations of Nrf2 mediate the antioxidant response element cytoprotective transcriptional response. Antoxid. Redox Signal. 23, 613–629. https://doi.org/10.1089/ars.2014.5962.
Yildiz-Unal, A., Korulu, S., Karabay, A., 2015. Neuroprotective strategies against calpain-mediated neurodegeneration. Neuropsychiatr. Dis. Treat. 11, 297–310. https://doi.org/10.2147/ndt.s78226.
Zatloukal, K., Stumptner, C., Fuchsbichler, A., Heid, H., Schnoelzer, M., Kenner, L., Kleinert, R., Prinz, M., Aguzzi, A., Denk, H., 2002. p62 is a common component of cytoplasmic inclusions in protein aggregation diseases. Am. J. Pathol. 160, 255–263. https://doi.org/10.1016/S0002-9440(10)64369-6.